Effect of annealing on the spectral and nonlinear optical characteristics of thin films of nano-ZnO

Litty Irimpan,[1,a)] D. Ambika,[2] V. Kumar,[2] V. P. N. Nampoori,[1] and P. Radhakrishnan[1]

[1]*International School of Photonics, Cochin University of Science and Technology, Cochin, Kerala 682022, India*
[2]*Centre for Materials for Electronics Technology, Thrissur-680 771, India*

The annealing effect on the spectral and nonlinear optical (NLO) characteristics of ZnO thin films deposited on quartz substrates by sol-gel process is investigated. As the annealing temperature increases from 300–1050 °C, there is a decrease in the band gap, which indicates the changes of the interface of ZnO. ZnO is reported to show two emission bands, an ultraviolet (UV) emission band and another in the green region. The intensity of the UV peak remains the same while the intensity of the visible peak increases with increase in annealing temperature. The role of oxygen in ZnO thin films during the annealing process is important to the change in optical properties. The mechanism of the luminescence suggests that UV luminescence of ZnO thin films is related to the transition from conduction band edge to valence band, and green luminescence is caused by the transition from deep donor level to valence band due to oxygen vacancies. The NLO response of these samples is studied using nanosecond laser pulses at off-resonance wavelengths. The nonlinear absorption coefficient increases from 2.9×10^{-6} to 1.0×10^{-4} m/W when the annealing temperature is increased from 300 to 1050 °C, mainly due to the enhancement of interfacial state and exciton oscillator strength. The third order optical susceptibility $\chi^{(3)}$ increases with increase in annealing temperature (T) within the range of our investigations. In the weak confinement regime, $T^{2.4}$ dependence of $\chi^{(3)}$ is obtained for ZnO thin films. The role of annealing temperature on the optical limiting response is also studied. © *2008 American Institute of Physics*. [DOI: 10.1063/1.2949400]

I. INTRODUCTION

The spectral and nonlinear optical (NLO) properties of semiconductors are the subject of much current theoretical and experimental interest.[1] Among the various NLO materials investigated, wide band gap semiconductors especially zinc oxide (ZnO) have attractive nonlinear properties that make them ideal candidates for NLO based devices. ZnO is a wide and direct band gap II-VI semiconductor with a band gap of 3.37 eV and a high exciton binding energy of 60 meV having many applications, such as solar cell, luminescent material, heterojunction laser diode, and ultraviolet (UV) laser.[2] The optical properties of this material are currently the subject of tremendous investigations, in response to the industrial demand for optoelectronic devices that could be operated at short wavelengths. Also, there is a significant demand for high NLO materials, which can be integrated into an optoelectronic device with a relatively small limiting threshold.
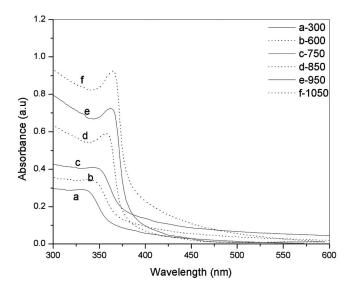
The ZnO bulk or nanoparticles have various luminescence transitions since different preparation techniques lead to varying structures and surface properties in ZnO. Generally, ZnO exhibits two kinds of emissions: one is at UV near band edge emission at approximately 380 nm and the other a visible deep level emission with a peak in the range of 450–730 nm.[3] Stoichiometric zinc oxide is an insulator that crystallizes with the wurtzite structure to form transparent needle-shaped crystals. The structure contains large voids that can easily accommodate interstitial atoms. Consequently, it is virtually impossible to prepare really pure crystals. Also, when these crystals are heated, they tend to lose oxygen.[4] For these reasons, the ZnO shows *n*-type semiconducting properties with many defects, such as lack of oxygen and excess of zinc. It is known that visible luminescence is mainly due to defects that are related to deep level emissions, such as Zn interstitials and oxygen vacancies. Vanheusden *et al.*[5] found that oxygen vacancies are responsible for the green luminescence in ZnO. Oxygen vacancies occur in three different charge states: the neutral oxygen vacancy (V_O^0), the singly ionized oxygen vacancy (V_O^*), and the doubly ionized oxygen vacancy (V_O^{**}) of which only V_O^* can act as the so-called luminescent center.[6]

ZnO films grown on silicon, sapphire, LiNbO$_3$, GaAs, and quartz substrates have been studied and the electrics, photoluminescence (PL), optical absorption, and optical nonlinearities have been investigated.[7] The substrate temperature, oxygen partial pressure, and post-treatments may significantly influence the structure and optical properties of the films, since the electrical and optical properties are strongly affected by the interface and the microstructure of the films. In this article, we present the effect of annealing on the spectral and NLO properties of the ZnO films on quartz substrates annealed within the temperature range of 300–1050 °C.

II. EXPERIMENT

The ZnO films are deposited on quartz substrates at room temperature using the technique of spin coating. A

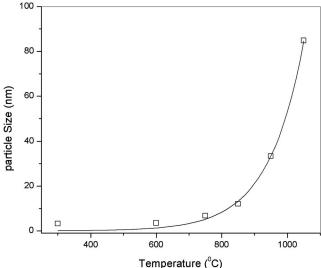
a)Electronic mail: littyirimpan@yahoo.co.in.

104, 033118-1

FIG. 1. Absorption spectra of ZnO thin films at different annealing temperatures.

FIG. 2. Variation of particle size deduced from absorption spectra as a function of annealing temperature for ZnO thin films.

stable hydrolyzed solution is prepared using stoichiometric quantities of zinc acetate dissolved in isopropyl alcohol, and the solution is used for spin coating ZnO thin films on quartz substrates at 2000 rpm. The series of samples are then dried at 110 °C for half an hour and then placed in a furnace for annealing. The samples are annealed at temperatures of 300, 600, 750, 850, 950, and 1050 °C and marked as *a*-300, *b*-600, *c*-750, *d*-850, *e*-950, and *f*-1050, respectively. The samples are held at each temperature for 3 h in air and then cooled to room temperature slowly.

The ZnO thin films are characterized by optical absorption measurements recorded using a spectrophotometer (JascoV-570 UV/VIS/IR), and the fluorescence emission measurements are recorded using a Cary Eclipse fluorescence spectrophotometer (Varian-Cary eclipse-06023419). The nonlinear absorption and refraction are investigated using *z* scan technique at the wavelength of 532 nm, in which a nanosecond Nd:yttrium aluminum garnet laser (Spectra Physics LAB-1760) with a pulse duration of 7 ns and repetition rate of 10 Hz is employed.[8] In the *z* scan, the laser beam is focused using a lens and the sample is translated along the laser beam axis (called the *z* direction) so that it passes through the focal point ($z=0$) during the motion. For each *z* value, the laser intensity is different at the sample and the sample transmission for different *z* values is measured. The transmitted beam energy, reference beam energy, and their ratio are measured simultaneously by an energy ratio meter (Rj7620, Laser Probe Corp.) having two identical pyroelectric detector heads (Rjp735). The effect of fluctuations of laser power is eliminated by dividing the transmitted power by the power obtained at the reference detector. Nonlinear absorption and refraction coefficients can be extracted from open and closed aperture *z* scan experiments, respectively, as described by Bahae *et al.*[9]

III. RESULTS AND DISCUSSION

Figure 1 gives the room temperature absorption spectra of the ZnO thin films. The excitonic peak is found to be

blueshifted (370–350 nm), with a decrease in particle size with respect to that of bulk ZnO, and this could be attributed to the confinement effects. By the quantum size effect in nanosized semiconductors, the band gap increases when the size of the particle is decreased, resulting in a blueshift of the absorption bands. The pronounced dependence of the absorption band gap on the size of ZnO nanocrystals is used to determine the particle size. An order of magnitude estimate of the particle size is possible from the absorption spectra. To get a precise measurement of the shift, the first derivative curve of the absorption spectrum is taken and the point of inflection is taken as the absorption edge. From the shift of absorption edge, the size of the dots is calculated.[10] The ZnO crystallite size increases exponentially from about 4 to 85 nm with the rise of the annealing temperature from 300 to 1050 °C, as shown in Fig. 2.

When the crystallite size is reduced to the order of an exciton Bohr radius a_B, quantum size effects appear and drastic changes in optical properties are expected. The quantum confinement effect in semiconductor nanocrystals can be classified into two regimes, i.e., strong and weak confinement regimes, according to the ratio of nanocrystal radius R to a_B.[1] NLO properties in nanocrystals have also been investigated for the corresponding confinement regimes. In the strong confinement regime, the photoexcited electron and hole are individually confined. Theoretical and experimental works have revealed that the state-filling effect accounts for the nonlinearity in this regime.[11] The size dependence of third order susceptibility $\chi^{(3)}$ has also been studied, but the results are inconsistent; a larger nonlinear susceptibility for a larger size has been found for CdS_xSe_{1-x} nanocrystals using the saturation spectroscopy and degenerate four-wave mixing (DFWM) measurements, while Roussignol *et al.* have shown that larger $\chi^{(3)}$ values are obtained with decreasing sizes.[11]

In the weak confinement regime, the Coulomb interaction between the electron and hole yields an exciton, and it is confined as a quasiparticle. The nonlinearity arises from the exciton-exciton interaction, which results in the deviation
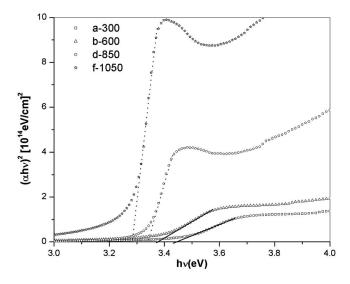
FIG. 3. Optical band gap of ZnO thin films at different annealing temperatures.

FIG. 4. Fluorescence spectra of ZnO thin films at different annealing temperatures for an excitation wavelength of 325 nm.

from harmonicity of the bosonlike exciton within the nanocrystal, and the size dependent enhancement of nonlinear susceptibility is investigated theoretically and experimentally.[12,13] Theoretical studies have shown that the confinement of excitonic envelope wave function due to the infinite barrier potential gives rise to the enhancement in oscillator strength for an exciton within the nanocrystal by a factor of R^3/a_B^3, and hence $\chi^{(3)}$ depends on the crystallite size. Such a giant oscillator strength effect has been confirmed for CuCl nanocrystals; the radiative decay rate of confined excitons is proportional to $R^{2.1}$ for the glass matrix and R^3 for the NaCl crystal matrix.[14] The validity of the size dependent enhancement effect has been limited by the long wavelength approximation, and a nonlocal theory applicable to the mesoscopic system larger than the wavelength has been developed.[13] The important role of the giant oscillator strength effect in the size dependent enhancement of nonlinearity has been experimentally shown for CuCl nanocrystals.[14] In ZnO, the exciton Bohr radius is 2 nm, which is roughly four times that of CuCl, and one can investigate confinement effects and size dependence of $\chi^{(3)}$ over a wide range of crystallite sizes.[15] In this study, as the annealing temperature increases from 300 to 1050 °C, the average particle size of ZnO increases from 4 to 85 nm, and hence it comes under the weak confinement regime.

The direct band gap of ZnO thin films is estimated from the graph of $h\nu$ vs $(\alpha h\nu)^2$ for the absorption coefficient α that is related to the band gap E_g as $(\alpha h\nu)^2 = k(h\nu - E_g)$, where $h\nu$ is the incident light energy and k is a constant. Extrapolation of the linear part until it intersects the $h\nu$ axis gives E_g. The optical band gap (E_g) is found to be temperature dependent, and there is a decrease in the band gap of the semiconductor with an increase in the annealing temperature, as shown in Fig. 3. As the films are annealed at a higher temperature, the crystallites begin to move and tend to agglomerate easily. As a result, the band gaps of the nanocomposites decrease with increasing annealing temperature. The shift of band gap energy is related to the structural property. Since ZnO thin film has a tensile built-in strain, the tensile
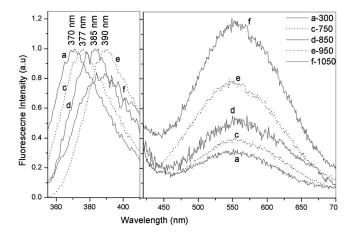
strain in ZnO can be relaxed by providing sufficient thermal energy. If the tensile strain is relaxed, the band gap energy is decreased. The total change in the band gap of the material is simultaneously contributed by shifts of the valence and the conduction band edges away from each other. In general, the shift of the top of the valence band (TVB) is not the same as that of the bottom of the conduction band (BCB). Moreover, though few in number, there are recent studies that report the individual shifts in TVB and BCB as a function of the size employing various forms of high-energy spectroscopies, such as the photoemission and x-ray absorption spectroscopies.[16] Thus, it is desirable to compute these shifts of the individual band edges with the size of the nanocrystallite. The shifts of the band edges decrease smoothly to zero for large sized nanocrystals in every case, and the shift in the BCB is, in general, much larger compared to the shift in the TVB for any given size of the nanocrystal. This indicates that the shifts in the total band gap as a function of the nanocrystal size are always dominated by the shifts of the conduction band edge in these systems. A larger shift for the BCB is indeed expected in view of the fact that the band edge shifts are related inversely to the corresponding effective masses, and the effective mass of the electron is always much smaller than that of the hole in these II-VI semiconductors. From these band edge shifts, the electronic structure as a function of the nanocrystallite size can be calculated for semiconductors.[16] The band gap is found to vary in the range of 3.28–3.44 eV for the range of annealing temperatures from 300–1050 °C and is in agreement with the reported value.[17] Film thickness is evaluated to be in the range of 60–100 nm from the interference bands in the transmittance spectra of the films on quartz substrates using the envelope method.[18]

Figure 4 shows the PL spectra of ZnO thin films annealed at different temperatures from 300–1050 °C. Two emission bands are present, and also an UV emission band and another in the green region. The UV emission band is assigned to a direct *band gap* transition. As the annealing temperature increases, this UV band undergoes a redshift with an increase in particle size as in the case of absorption spectrum. Such size dependent optical properties of semiconductor particle suspensions in the quantum regime are well
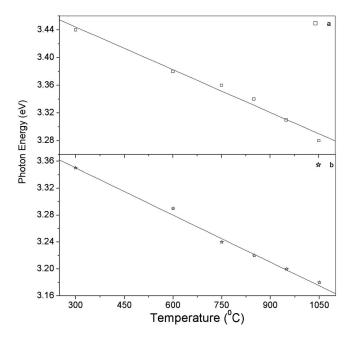
FIG. 5. The dependence of annealing temperature on (a) band gap (b) band to band emission.

known, and similar observations have previously been made for several quantum particle systems.[3] For the intrinsic luminescence of ZnO nanoparticles, it is generally known that the formation of nanoparticles causes a redshift in the PL spectra due to quantum size effect.[3] The UV emission peak is shifted from 3.34 to 3.18 eV due to the shift of the optical band gap from 3.44 to 3.28 eV, and it clearly indicates that the origin of UV emission is near the band edge emission. Figure 5(a) shows the band gap change as a function of the annealing temperature. Figure 5(b) shows the energy of the band to band transition as a function of the annealing temperature. The redshift in the UV emission with annealing temperature closely follows the redshift in the band edge, indicating that the two are related. Mean cluster size could be principally derived from the absorption measurements, and the ZnO crystallite size increases exponentially from about 4 to 85 nm with the rise of the annealing temperature from 300 to 1050 °C, as shown in Fig. 2. This allows us to reconstruct the size distribution curves in the fluorescence spectrum.[3] The intensity of the UV emission remains the same, whereas the intensity of the green emission increases with annealing temperature. However, there is a decrease in the UV luminescence intensity at the annealing temperature of 1050 °C, and this can be mainly due to the formation of interstitial vacancies when the films annealed at a high temperature.

As the annealing temperature increases, the intensity of UV emission of ZnO films remains unaffected, whereas the intensity of green luminescence increases. The intensity of green emission becomes even stronger than that of UV emission at an annealing treatment of 1050 °C. The most prominent peak position is changed from UV to green emission after annealing treatment at 1050 °C. The intensity variation of green luminescence is systematically studied as a function of annealing temperatures in order to investigate the emission mechanism. The increase of green luminescence after

annealing treatment suggests the increase of singly ionized oxygen vacancies according to the result of Vanheusden *et al.*[5]

In ZnO, oxygen has tightly bound $2p$ electrons and Zn has tightly bound $3d$ electrons, which sense the nuclear attraction efficiently. The first principal calculation found that the Zn_{3d} electrons strongly interact with the O_{2p} electron in ZnO.[19] Since the center energy of the green peak is smaller than the band gap energy of ZnO (3.37 eV), the visible emission cannot be ascribed to the direct recombination of a conduction electron in the Zn_{3d} band and a hole in the O_{2p} valence band. The green emission must be related to the local level in band gap.

Surface states can contribute green emission in ZnO.[20] For the uncapped ZnO nanoparticles, there exist abundant surface defects, and the valence band hole can be trapped by the surface defects and then tunnels back into oxygen vacancies containing one electron to form V_O^{**} recombination center. The recombination of a shallowly trapped electron with a deeply trapped hole in a V_O^{**} center causes visible emission. The most likely explanation for the green luminescence involves multiple defects and/or defect complexes and the major part of the visible emission originates from the centers at the surface of the nanostructure. Xu *et al.*[21] calculated the levels of various defects including complex defects $V_O:Zn_i$ and $V_{Zn}:Zn_i$. They found no states within the gap from $V_{Zn}:Zn_i$, while for $V_O:Zn_i$, two levels 1.2 and 2.4 eV above the valence band were found, so this type of defect represents a possible candidate for green emission in ZnO.

Due to its *n*-type semiconductor nature, the most defects in ZnO are Zn interstitials and oxygen vacancies. The crystal structure of ZnO contains large voids that can easily accommodate interstitial atoms.[4] These Zn interstitials in ZnO are easily ionized, electrons produced by ionized Zn interstitials contribute to electrical conductivity and the number of Zn interstitials decreases probably due to Zn evaporation at increasing annealing temperatures. However, the number of oxygen vacancies increases with increase in annealing temperature. Therefore, the intensity of green luminescence is increased when annealing temperature is increased. ZnO nanopowders and thin films also showed green luminescence after they were annealed in oxygen, nitrogen, or air.[22] The appearance of a strong green emission is ascribed to the formation of oxygen vacancy defects or antisite defects (O_{Zn}). There exist many oxygen vacancies on the surface of the ZnO annealed in Ar at 900 °C and show emission peak at 490 nm, while the ZnO annealed in O_2 at 900 °C exhibits emission peak at 530 nm.[22] Thus, in our present studies, the emission at 530 nm may have originated from the antisite defects (O_{Zn}).

The inset of Fig. 6 shows the variation of green PL intensity depending on annealing temperature. The intensity of green emission dramatically increases above an annealing temperature of 750 °C. Figure 6 is an Arrhenius plot to calculate the activation energy. The activation energies are estimated from the Arrhenius equation based on a plot of the PL intensity of green emission versus annealing temperature.[23] The activation energy (E_A) is derived using the equation
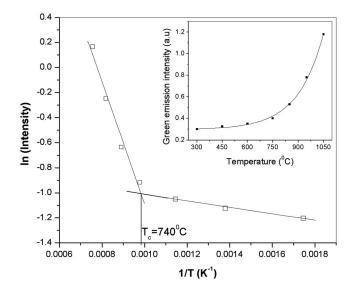
FIG. 6. Arrhenius plot to calculate the activation energy from the variation of green PL intensity with annealing temperature.

$$PL_i = PL_{i0} \exp\left(\frac{-E_A}{kT}\right), \qquad (1)$$

where PL_i is the PL intensity at annealing temperature of T, PL_{io} is the pre-exponential factor, and k is the Boltzmann constant. The plot shows a break at a transition temperature of 740 °C, suggesting a change in mechanism from a low temperature (300–650 °C) activated process to a high temperature (750–1050 °C) activated process. An indication of this change in process exists in the literature.[23] The practical significance of this observation is that it would now require caution in extrapolating the high temperature data to represent behavior in the low temperature regime. In the high temperature regime, the calculated activation energy is 0.42 eV; in the low temperature regime, the calculated activation energy is 0.22 eV. This value reasonably agrees with the result reported by Gavryushin *et al.*[24] From these results, it is considered that many oxygen vacancies are generated due to the large lattice mismatch between the film and the substrate and provide high surface energy during the annealing process at and above the transition temperature of 740 °C. Therefore, the green emission related to the donor level is dominant due to the increase in oxygen vacancies. It suggests that the activation energy of 0.42 eV is related to the dominance of this donor level.

Figure 7 shows the emission mechanism of UV and visible luminescence of ZnO films. UV luminescence is caused by the transition from near conduction band edge to valence band. As temperature increases, the shift of UV luminescence is observed from 3.34 to 3.18 eV due to the shift of the optical energy gap from 3.44 to 3.28 eV. The green luminescence is mainly due to surface state effects. The UV luminescence center is not related to the visible luminescence center. Based on these results, it can be concluded that the green luminescence of ZnO is not due to the transition from near band edge to deep acceptor level in ZnO, but is mainly due to the transition from deep donor level by oxygen vacancies in ZnO to valence band. If green luminescence is related
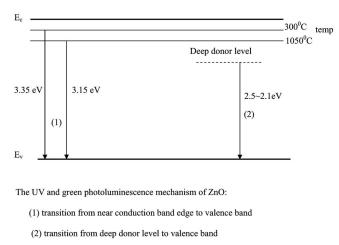

FIG. 7. The UV and green PL mechanism of ZnO: (1) transition from near conduction band edge to valence band and (2) transition from deep donor level to valence band.

to the deep acceptor level, UV luminescence should decrease as green luminescence increased. These results reveal that the mechanism of green luminescence in ZnO is by the transition from deep donor level resulting from the oxygen vacancies to valence band.

Figure 8 gives the open aperture z scan traces of ZnO films annealed at different temperatures at a typical fluence of 300 MW/cm². The open aperture curve exhibits a normalized transmittance valley, indicating the presence of induced absorption in the ZnO thin films. The data are analyzed by using the procedure described by Bahae *et al.*[25] for two photon absorption (TPA) processes, and the nonlinear absorption coefficient β is obtained by fitting the experimental z scan plot to Eq. (2).

$$T(z) = \frac{C}{q_0\sqrt{\pi}} \int_{-\infty}^{\infty} \ln(1 + q_0 e^{-t^2})dt \quad \text{where} \quad q_o(z,r,t)$$

$$= \beta I_o(t) L_{\text{eff}}. \qquad (2)$$

Here, $L_{\text{eff}} = 1 - e^{-\alpha l}/\alpha$ is the effective thickness with linear
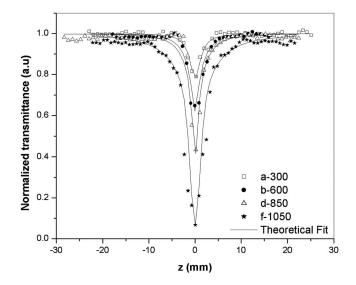

FIG. 8. The open aperture z scan traces of ZnO thin films at different temperatures at a typical fluence of 300 MW/cm².

TABLE I. The measured values of nonlinear absorption coefficient, refractive index, and third order susceptibility of ZnO thin films at an intensity of 300 MW/cm^2 for an irradiation wavelength of 532 nm at different annealing temperatures.

Annealing temperature °C	β (10^{-6} m/W)	n_2 (10^{-5} esu)	Im($\chi^{(3)}$) (10^{-6} esu)	Re $\chi^{(3)}$ (10^{-6} esu)	$\|\chi^{(3)}\|$ 10^{-6} esu
300	2.9	1.1	0.1	2.3	2.3
600	6.9	1.5	0.3	3.1	3.2
750	13.8	2.1	0.6	4.5	4.6
850	19	2.8	0.8	6	6.1
950	51.8	3.5	2.2	7.5	7.8
1050	103.7	5.9	4.5	12.6	13.4

absorption coefficient α, nonlinear absorption coefficient β, and I_o is the irradiance at focus. The solid curves in Fig. 8 are the theoretical fit to the experimental data. The imaginary part of third-order susceptibility Im $\chi^{(3)}$ is related to β through the equation Im $\chi^{(3)} = n_o^2 \varepsilon_o c^2 \beta / \omega$, where $n_o = 2.008$ is the linear refractive index of ZnO, ε_o is the permittivity of free space, c is the velocity of light in vacuum, and ω is the angular frequency of the radiation used. The experimentally obtained values of nonlinear absorption coefficient β at an intensity of 300 MW/cm^2 are shown in Table I

Figure 9 gives the closed aperture z scan traces of ZnO thin films at different temperatures at a fluence of 300 MW/cm^2. The closed aperture curve exhibited a peak-to-valley shape, indicating a negative value of the nonlinear refractive index n_2. For samples with sizable refractive and absorptive nonlinearities, closed aperture measurements contain contributions from both the intensity dependent changes in the transmission and in the refractive index.[25] By dividing the normalized closed aperture transmittance by the corresponding normalized open aperture data, we can retrieve the phase distortion created due to the change in refractive index.

It is observed that the peak valley of closed aperture z scan satisfied the condition $\Delta z \sim 1.7\, z_0$, thus confirming the presence of cubic nonlinearity.[25] The value of the difference
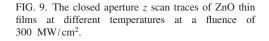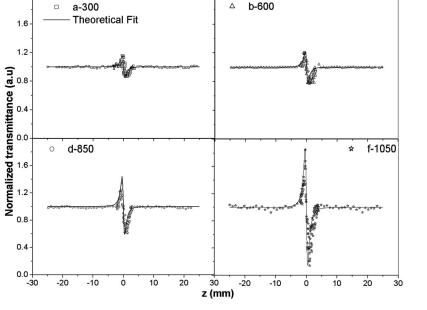
between the peak and valley transmittance ΔT_{p-v} can be obtained by the best theoretical fit from the results of the divided z scan curve. The nonlinear refractive index n_2 and the real part of nonlinear susceptibility Re $\chi^{(3)}$ are given respectively by Eq. (3).

$$n_2(esu) = \frac{Cn_0}{40\pi^2} \frac{\lambda\Delta T_{p-v}}{0.812(1-S)^{0.25}L_{\text{eff}}I_0} \quad \text{and} \quad \text{Re } \chi^{(3)}$$

$$\times(esu) = \frac{n_0 n_2(esu)}{3\pi}. \tag{3}$$

The nonlinear refractive index n_2 and real part of $c^{(3)}$ evaluated using the above equations are tabulated in Table I From the real and imaginary part of $c^{(3)}$, the modulus of third order susceptibility is calculated and is tabulated in Table I

The enhancement of NLO properties with increasing dimension in accordance with increasing annealing temperature in the weak confinement regime essentially originates from the size dependent enhancement of oscillator strength of coherently generated excitons. Since the exciton is confined in a quantum dot, the confinement of excitonic wave function is expected to give rise to enhancement of the oscillator strength per quantum dot by a factor of R^3/a_B^3.[12] This size dependent oscillator strength was experimentally con-

FIG. 9. The closed aperture z scan traces of ZnO thin films at different temperatures at a fluence of 300 MW/cm^2.
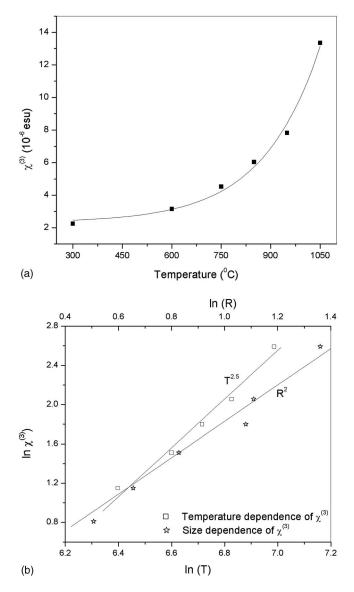
FIG. 10. (a) Variation of third order susceptibility as a function of annealing temperature. (b) Dependence of third order susceptibility as a function of annealing temperature and particle size for ZnO thin films. The straight lines indicate $T^{2.5}$ and R^2 dependence.

firmed in CuCl quantum dots.[14] Such a giant oscillator strength effect will result in an enhancement of the nonlinear susceptibility.

Figure 10(a) shows the variation of $\chi^{(3)}$ as a function of annealing temperature. The data show an exponential increase in $\chi^{(3)}$ values with increasing temperature and the values ranging from 2.3×10^{-6} to 1.3×10^{-5} esu for $T = 300 - 1050$ °C. For the samples annealed below 750 °C, the absolute value of $\chi^{(3)}$ does not change significantly, but for the ones annealed above 750 °C, the $\chi^{(3)}$ value increases rapidly with the increase in the annealing temperature. At lower temperatures and for films with small size, $\chi^{(3)}$ is small, indicating that it is a third order effect resulting from TPA. For films of larger particle size and at higher temperatures, $\chi^{(3)}$ becomes very large, indicating the occurrence of higher order nonlinear processes, such as free-carrier absorption. The free-carrier lifetime of ZnO is reported to be 2.8 ns.[26] Hence, there is a strong possibility that the 7 ns pulses

used in the present study is exciting the accumulated free carriers generated by TPA by the rising edge of the pulse. For samples annealed at higher temperatures, the $\chi^{(3)}$ value increases rapidly because of the interdiffusion of the SiO_2 substrates and ZnO films.[17] For samples annealed at 1050 °C, the $\chi^{(3)}$ value is one order of magnitude larger than that at 950 °C due to the interfacial state enhancement. Furthermore, as the ZnO microcrystallites are melted into the SiO_2 substrate, the local field effect and the interband transition of electrons from the interfacial state to the unoccupied state near the Fermi level will greatly enhance the nonlinear absorption.[27] In order to obtain the annealing temperature and particle size dependence of the third order susceptibility, $\ln(T)$ and $\ln(R)$ are plotted against $\ln(\chi^{(3)})$ and are shown in Fig. 10(b). When we apply a least-squares fit, a temperature dependence of $T^{2.4}$ and a size dependence of R^2 is obtained, indicating an enhancement of more than two orders of magnitude. This dependence is in good agreement with that observed for CdS, CuCl, and CuBr nanocrystals and ZnO colloids.[28,29]

The nonlinear absorption coefficient is reported to increase from 1.2×10^2 to 1.1×10^3 cm/GW when the annealing temperature rises from 950 to 1050 °C for ZnO microcrystalline films developed by sputtering technique.[17] The enhancement of nonlinear coefficients for our thin nanocrystalline films compared to microcrystalline films of ZnO is attributed to the nanosized structure of the films. It has been reported that the reduced dimensionality of the particles resulted in considerable enhancement of the second order susceptibility $\chi^{(2)}$ in thin films of ZnO.[30] Similar results in the third order nonlinear parameters are evident in our measurements also. The values of $\chi^{(3)}$ measured at room temperature by DFWM technique on CuBr nanocrystals range from 8×10^{-11} to 1.1×10^{-9} esu for $R = 2.7 - 42$ nm and are comparable to the results presented here.[28] In this paper, we report the experimental evidence for the enhancement of third order nonlinear susceptibility due to the size dependent oscillator strength of confined excitons, which was theoretically predicted by Hanamura.[12] Recently significant ($\sim$500 times) enhancement of nonlinear refractive index with respect to the bulk value has been observed for polymer capped ZnO nanocrystals with an estimated average size of 4 nm.[30] The third order NLO response of these poly vinyl pyrrolidone (PVP) -capped ZnO nanoparticles in a dilute solution was reported to be significantly larger and was of the order of 6.3×10^{-11} esu. This value is at least two orders of magnitude greater than that of the bulk ZnO. This remarkable enhancement in the third order NLO response may be related to the exciton confinement and optical Stark effects.[31]

The values of $\chi^{(3)}$ measured at room temperature by femtosecond DFWM technique on ZnO microcrystalline thin films range from 10^{-4} to 10^{-7} esu.[32] The β values obtained are quite high and are of the same order of magnitude as those obtained for ZnO–Cu and ZnO–Mg nanocomposite films.[33] Thus, the real and imaginary parts of third order NLO susceptibility measured by the z scan technique revealed that the ZnO colloids investigated in the present study have good NLO response and could be chosen as ideal candidates with potential applications in nonlinear optics.
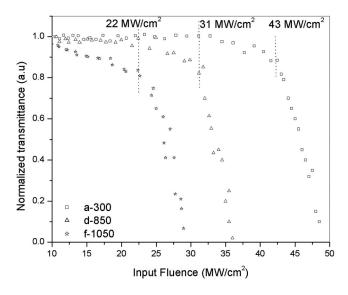
FIG. 11. Optical limiting curves of ZnO thin films at different annealing temperatures.

Recently, nanomaterials have drawn significant attention as optical limiters[34] for eyes or for sensor protection from laser terror in homeland or agile laser threats on the battlefield. Also, the NLO properties of nanomaterials are of great interest for optical switching, pulse power shaping of optical parametric oscillator/optical parametric generator, and other NLO applications. Optical power limiting is operated through the NLO processes of nanomaterials. However, the great potential of nanomaterials as optical power limiters has just begun to be recognized.

To examine the viability of nano-ZnO films as optical limiters, the nonlinear transmission of the film is studied as a function of input fluence. An important term in the optical limiting measurement is the limiting threshold. It is obvious that the lower the optical limiting threshold, the better the optical limiting material. Optical limiters are devices that transmit light at low input fluences or intensities, but become opaque at high inputs. The optical limiting property occurs mostly due to absorptive nonlinearity, which corresponds to the imaginary part of third order susceptibility.[35] From the value of fluence at focus, the fluence values at other positions could be calculated using the standard equations for Gaussian beam waist. Such plots represent a better comparison of the nonlinear absorption or transmission in these samples and are generated from z scan traces. Figure 11 illustrates the influence of annealing temperature on the optical limiting response.

The fluence value corresponding to the onset of optical limiting (optical limiting threshold) is found to be high in the case of ZnO films annealed at a temperature of 300 °C (43 MW/cm^2) in comparison with the ZnO films annealed at a temperature of 850 °C (31 MW/cm^2) and ZnO films annealed at a temperature of 1050 °C (22 MW/cm^2). These values are comparable to the reported optical limiting threshold for ZnO nanocolloids of different particle size.[29,36] The arrow in the figure indicates the approximate fluence at which the normalized transmission begins to deviate from linearity. Annealing temperature, and hence particle size, has

a significant effect on the limiting performance of ZnO films. Increasing the annealing temperature reduces the limiting threshold and enhances the optical limiting performance. From the measured values of β for the ZnO films, it can be seen that the film annealed at a higher temperature and having larger particle size is a better nonlinear absorber and hence a good optical limiter.

IV. CONCLUSIONS

The annealing effect on the spectral and NLO characteristics of ZnO thin films deposited on quartz substrates by sol-gel process is investigated. As the annealing temperature increases from 300–1050 °C, there is a decrease in the band gap, which indicates the changes of the interface of ZnO. In the fluorescence spectra, we have observed two principal bands: (1) a UV band and (2) a visible band. The UV band has been assigned to the band gap fluorescence of clusters of different sizes. This allows us to reconstruct the size distribution curves from fluorescence spectroscopy. The intensity of UV peak remains the same while the intensity of the visible peak increases with increase in annealing temperature. The luminescence mechanism can be used to control the optical properties of ZnO for optical device applications. The mechanism of the luminescence suggests that UV luminescence of ZnO thin films is related to the transition from conduction band edge to valence band, and green luminescence is caused by the transition from deep donor level resulting from oxygen vacancies to valence band. The activation energy derived from the variation of green emission intensity is 0.42 eV. The NLO response of these samples is studied using nanosecond laser pulses at 532 nm for optical limiting applications. The nonlinear susceptibility increases from 2.3 $\times 10^{-6}$ to 1.3×10^{-5} esu when the annealing temperature rises from 300 °C to 1050 °C, mainly due to the enhancement of interfacial state and exciton oscillator strength. We have experimentally demonstrated optical nonlinearity as a function of temperature, and a $T^{2.4}$ dependence of nonlinear susceptibility has been obtained for thin films of nano-ZnO. Optical limiting response is temperature dependent and the film annealed at higher temperature and having larger particle size is a better nonlinear absorber, and hence, a good optical limiter.

[1] Y. Kayanuma, Phys. Rev. B **38**, 9797 (1988).
[2] L. Irimpan, V. P. N. Nampoori, and P. Radhakrishnan, J. Appl. Phys. **103**, 094914 (2008).
[3] L. Irimpan, A. Deepthy, B. Krishnan, V. P. N. Nampoori, and P. Radhakrishnan, J. Appl. Phys. **102**, 063524 (2007).
[4] L. V. Azaroff, *Introduction to Solids* (McGraw-Hill, New York, 1960), pp. 371–372.
[5] K. Vanheusden, W. L. Warren, C. H. Seager, D. R. Tallant, J. A. Voigt, and B. E. Gnade, J. Appl. Phys. **79**, 7983 (1996).
[6] W. Li, D. Mao, F. Zhang, X. Wang, X. Liu, S. Zou, Y. Zhu, Q. Li, and J. Xu, Nucl. Instrum. Methods Phys. Res. B **169**, 59 (2000).
[7] J. H. Lin, Y. J. Chen, H. Y. Lin, and W. F. Hsieh, J. Appl. Phys. **97**, 033526 (2005).
[8] L. Irimpan, A. Deepthy, B. Krishnan, V. P. N. Nampoori, and P. Radhakrishnan, Appl. Phys. B: Lasers Opt. **90**, 547 (2008).

9M. Sheik-Bahae, A. A. Said, T. H. Wei, D. J. Hagan, and E. W. Van Stryland, IEEE J. Quantum Electron. **26**, 760 (1990).

10R. Viswanatha, S. Sapra, B. Satpati, P. V. Satyam, B. N. Dev, and D. D. Sharma, J. Mater. Chem. **14**, 661 (2004).

11P. Roussignol, D. Ricard, and C. Flytzanis, Appl. Phys. B: Lasers Opt. **51**, 437 (1990).

12E. Hanamura, Phys. Rev. B **37**, 1273 (1988).

13H. Ishihara and K. Cho, Phys. Rev. B **42**, 1724 (1990).

14T. Itoh, M. Furumiya, and C. Gourdon, Solid State Commun. **73**, 271 (1990).

15H. L. Cao, X. F. Qian, Q. Gong, W. M. Du, X. D. Ma, and Z. K. Zhu, Nanotechnology **17**, 3632 (2006).

16S. Sapra and D. D. Sarma, Phys. Rev. B **69**, 125304 (2004).

17Y. B. Han, J. B. Han, S. Ding, D. J. Chen, and Q. Q. Wang, Opt. Express **13**, 9211 (2005).

18J. C. Manifacier, J. Gasiot, and J. P. Fillard, J. Phys. E **9**, 1002 (1976).

19P. Schroer, P. Kruger, and J. Pollmann, Phys. Rev. B **47**, 6971 (1993).

20D. Li, Y. H. Leung, A. B. Djurisic, Z. T. Liu, M. H. Xie, S. L. Shi, S. J. Xu, and W. K. Chan, Appl. Phys. Lett. **85**, 1601 (2004).

21P. S. Xu, Y. M. Sun, C. S. Shi, F. Q. Xu, and H. B. Pan, Nucl. Instrum. Methods Phys. Res. B **199**, 286 (2003).

22J. Z. Wang, G. T. Du, Y. T. Zhang, B. J. Zhao, X. T. Yang, and D. L. Liu, J. Cryst. Growth **263**, 269 (2004).

23T. K. Gupta and W. D. Straub, J. Appl. Phys. **68**, 845 (1990).

24V. Gavryushin, G. Raciukaitis, D. Judozbalis, A. Kazlauskas, and V. Kubertavicius, J. Cryst. Growth **138**, 924 (1994).

25M. S. Bahae, A. A. Said, and E. W. van Stryland, Opt. Lett. **14**, 955 (1989).

26X. J. Zhang, W. Ji, and S. H. Tang, J. Opt. Soc. Am. B **14**, 1951 (1997).

27R. G. Xie, J. Q. Zhuang, L. L. Wang, W. S. Yang, D. J. Wang, T. J. Li, and J. N. Yao, Gaodeng Xuexiao Huaxue Xuebao **24**, 2086 (2003).

28Y. Li, M. Takata, and A. Nakamura, Phys. Rev. B **57**, 9193 (1998).

29L. Irimpan B. Krishnan, A. Deepthy, V. P. N. Nampoori, and P. Radhakrishnan, J. Appl. Phys. **103**, 033105 (2008).

30G. Wang, G. T. Kiehne, G. K. L. Wong, J. B. Ketterson, X. Liu, and R. P. H. Chang, Appl. Phys. Lett. **80**, 401 (2002).

31H. Cao, J. Y. Xu, E. W. Seelig, and R. P. H. Chang, Appl. Phys. Lett. **76**, 2997 (2000).

32L. Guo, S. Yang, C. Yang, P. Yu, J. Wang, W. Ge, and G. K. L. Wong, Appl. Phys. Lett. **76**, 2901 (2000).

33A. Nakamura, H. Yamada, and T. Tokizaki, Phys. Rev. B **40**, 8585 (1989).

34C. S. Suchand Sandeep, R. Philip, R. Satheeshkumar, and V. Kumar, Appl. Phys. Lett. **89**, 063102 (2006).

35Y. Sun, J. E. Riggs, K. B. Henbest, and R. B. Martin, J. Nonlinear Opt. Phys. Mater. **9**, 481 (2000).

36F. M. Qureshi, S. J. Martin, X. Long, D. D. C. Bradley, F. Z. Heneri, W. J. Balu, E. C. Smith, C. H. Wang, A. K. Kar, and H. L. Anderson, Chem. Phys. **231**, 87 (1998).